

Haverford College

Haverford Scholarship

Faculty Publications

Physics

2001

Controlled creation of a carbon nanotube diode by a scanned gate

Marcus Freitag

Marko Radosavljevic

Yangxin Zhou

Walter Fox Smith

Haverford College, wsmith@haverford.edu

Follow this and additional works at: https://scholarship.haverford.edu/physics_facpubs

Repository Citation

Freitag, Marcus, et al. "Controlled creation of a carbon nanotube diode by a scanned gate." *Applied Physics Letters* 79.20 (2001): 3326-3328.

This Journal Article is brought to you for free and open access by the Physics at Haverford Scholarship. It has been accepted for inclusion in Faculty Publications by an authorized administrator of Haverford Scholarship. For more information, please contact nmedeiro@haverford.edu.

Controlled creation of a carbon nanotube diode by a scanned gate

Marcus Freitag, Marko Radosavljevic, Yangxin Zhou, A. T. Johnson, and Walter F. Smith

Citation: *Appl. Phys. Lett.* **79**, 3326 (2001); doi: 10.1063/1.1419055

View online: <http://dx.doi.org/10.1063/1.1419055>

View Table of Contents: <http://apl.aip.org/resource/1/APPLAB/v79/i20>

Published by the [American Institute of Physics](#).

Additional information on *Appl. Phys. Lett.*

Journal Homepage: <http://apl.aip.org/>

Journal Information: http://apl.aip.org/about/about_the_journal

Top downloads: http://apl.aip.org/features/most_downloaded

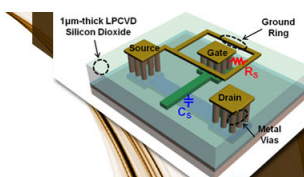
Information for Authors: <http://apl.aip.org/authors>

ADVERTISEMENT



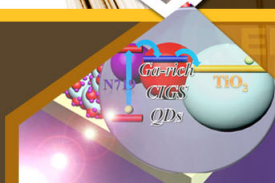
**EXPLORE WHAT'S
NEW IN APL**

SUBMIT YOUR PAPER NOW!



SURFACES AND INTERFACES

Focusing on physical, chemical, biological, structural, optical, magnetic and electrical properties of surfaces and interfaces, and more...



ENERGY CONVERSION AND STORAGE

Focusing on all aspects of static and dynamic energy conversion, energy storage, photovoltaics, solar fuels, batteries, capacitors, thermoelectrics, and more...

Controlled creation of a carbon nanotube diode by a scanned gate

Marcus Freitag, Marko Radosavljevic, Yangxin Zhou, and A. T. Johnson^{a)}

Department of Physics and Astronomy and Laboratory for Research on the Structure of Matter, University of Pennsylvania, Philadelphia, Pennsylvania 19104

Walter F. Smith

Department of Physics, Haverford College, Haverford, Pennsylvania 19041

(Received 27 June 2001; accepted for publication 7 September 2001)

We use scanning gate microscopy to precisely locate the gating response in field-effect transistors (FETs) made from semiconducting single-wall carbon nanotubes. A dramatic increase in transport current occurs when the device is electrostatically doped with holes near the positively biased electrode. We ascribe this behavior to the turn-on of a reverse biased Schottky barrier at the interface between the *p*-doped nanotube and the electrode. By positioning the gate near one of the contacts, we convert the nanotube FET into a rectifying nanotube diode. These experiments both clarify a longstanding debate over the gating mechanism for nanotube FETs and indicate a strategy for diode fabrication based on controlled placement of acceptor impurities near a contact. © 2001 American Institute of Physics. [DOI: 10.1063/1.1419055]

Single wall carbon nanotubes (SWNTs), which can be semiconducting or metallic,^{1–3} are promising nanoelectronic components. Semiconducting SWNTs work as molecular field-effect transistors (TUBEFET)⁴ that can be converted to diodic rectifiers by localized impurities⁵ or alkali dopants.⁶ Metallic SWNTs could serve as one-dimensional interconnects between molecular devices, carrying current densities up to 10⁹ A/cm². At low temperatures they show Coulomb blockade effects and act as single electron transistors.^{7,8} Finally, heterostructures of nanotubes with differing chiralities are expected to produce zero-dimensional on-tube devices.^{9,10}

Semiconducting SWNTs with diameters near 1.5 nm have a band gap near 0.5 eV. For an isolated tube, the Fermi level is expected to be at midgap, but gas exposure and other effects shift the chemical potential considerably. Semiconducting SWNTs exposed to atmosphere typically show hole transport.¹¹ *n*-type doping into the metallic regime occurs upon doping with potassium.^{12–14} Moreover, charge transfer between metal contacts and the nanotube shifts its chemical potential and leads to band bending in the nanotube. Band bending is predicted to occur over nanometer length scales for heavily doped nanotubes or micrometers for nearly depleted nanotubes.¹⁵

Contradictory models have been proposed to explain FET action in semiconducting nanotubes. Tans *et al.* suggested that the tube valence band was pinned at the Fermi level of the leads and “sagged” away from the contacts to produce a barrier to hole transport in the middle of the device.⁴ A fundamentally different model was proposed for the junction between crossed SWNTs, one metallic and one semiconducting.¹⁶ A Schottky barrier at the nanotube–nanotube contact was proposed, with the rest of the semiconducting nanotube doped to a conductive state.

Here we resolve this issue by directly probing the local field effect in a nanotube field-effect transistor using a scan-

ning gate microscope (SGM). The method has previously been used to reveal semiconducting areas in nanotube bundles,¹⁷ to image potential modulations along a semiconducting nanotube,^{18,19} and to study defects in metallic nanotubes.²⁰ We extend these earlier results by unambiguously locating gate-susceptible regions to demonstrate that Schottky barriers at the electrode–SWNT contacts produce much of the observed field-effect behavior. We also demonstrate that an appropriately biased SGM tip positioned near one contact converts the symmetric nanotube FET into a nanotube diode. This result complements and clarifies our group’s earlier observation of rectification induced by static impurities.⁵

TUBEFET devices are fabricated in one of two ways: (a) laser-ablation grown nanotubes are spun onto prefabricated submicron gold leads from a dichloroethane suspension or (b) nanotubes are grown catalytically by chemical vapor deposition (CVD)²¹ directly on the chip. Cr/Au electrical leads are fabricated on top of the nanotubes by *e*-beam lithography.²² Semiconducting nanotubes are identified by strong gating action. The two-probe, room-temperature low-voltage resistance of laser-grown TUBEFETs is above 100 MΩ, while CVD-grown samples have a resistance below 10 MΩ. This difference might be due to an insulating contamination layer on laser-grown nanotubes that have been suspended in solution. Another possibility is that the relatively low-temperature growth process ($T \sim 800^\circ\text{C}$) gives CVD-grown nanotubes a higher defect density, producing localized states that couple well to the leads. Despite the difference in the two-probe resistance, the qualitative results are the same for all samples.

In SGM (Fig. 1) a conductive tip with an applied potential is scanned under AFM-feedback in proximity to a nanotube device.^{23,24} In contrast to a static backgate that couples capacitively to the entire sample, the tip is a spatially localized gate whose position is varied at will. We use two modes of SGM operation. In “imaging mode,” a bias voltage is applied to the sample and the transport current recorded as a

^{a)}Electronic mail: cjohnson@physics.upenn.edu

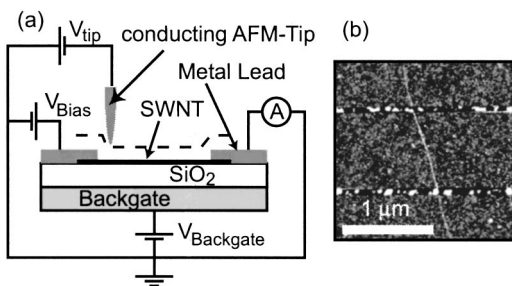


FIG. 1. (a) Schematic of the experiment. A conducting AFM probe is scanned above the TUBEFET. Voltages at the electrodes, the tip gate and the backgate are adjusted separately. The transport current through the device is measured. (b) AFM image of a TUBEFET sample grown by CVD with a nanotube diameter of 1.4 nm. The image has been flattened to increase the contrast of the nanotube.

function of tip position. This reveals precise locations where the current changes in the presence of the local “dopant” (the tip). In “spectroscopy mode,” the tip is fixed in place, and the transport current through the sample recorded as a function of bias voltage. In this mode we simulate device behavior in the presence of a local dopant.

Figure 2 shows SGM data of a CVD-grown TUBEFET. For imaging mode scans [Figs. 2(a) and 2(b)], the tip is biased at -2 V, and a bias of $+1$ V is applied to the left and right electrodes, respectively, while the other electrode is grounded. Strikingly, a pronounced gating action in each case is localized immediately at the contact from the SWNT

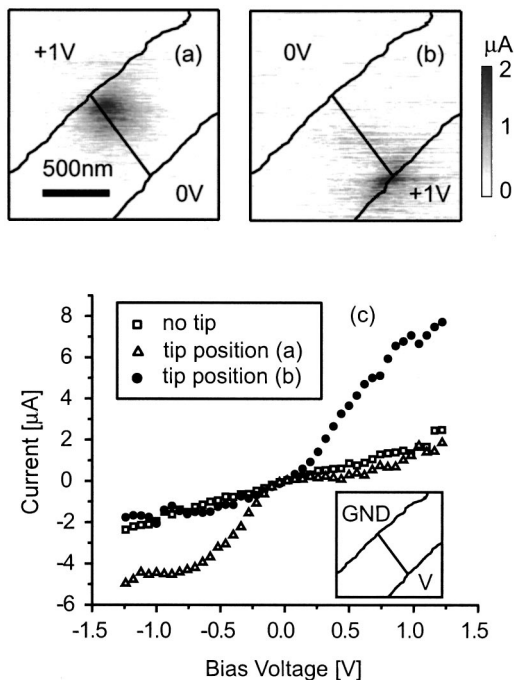


FIG. 2. Scanned gate microscopy on a CVD-grown TUBEFET. The tip potential is -2 V, and the backgate is grounded. (a) SGM image with the top-left electrode at $+1$ V bias and the bottom-right electrode grounded. The base-current level is subtracted. The electrodes and nanotube are sketched for clarity. (b) SGM image with the bias and ground connections reversed. In each case, the current is strongly enhanced when the tip gate is near the positively biased contact. (c) $I-V$ characteristics of the nanotube with and without tip gating. The bias is applied to the bottom-right electrode while the top-left electrode is grounded. Without tip gating (open squares), the $I-V$ is symmetric. With tip gating near the top-left or bottom-right contact (open triangles or filled circles), the $I-V$ is rectifying, with a sharp current increase when the electrode near the tip gate is positively biased.

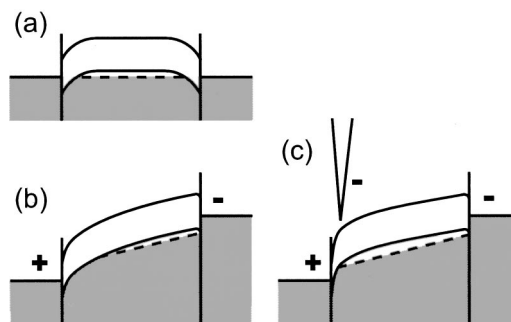


FIG. 3. Energy band diagrams for the TUBEFET. (a) Zero bias; (b) biased; (c) biased and tip-gated.

to the positively biased electrode, a behavior seen in more than ten samples grown by both CVD and laser. If the tip potential is reversed to $+2$ V, this predictable bias-dependent behavior no longer occurs. Instead we see irregularly distributed spots along the nanotube’s length where the current is suppressed, similar to earlier observations.¹⁸ In spectroscopy mode [Fig. 2(c)], $I-V$ curves were taken with the tip far away from the sample, near the top-left electrode, and near the bottom-right electrode (the tip voltage was -2 V). With no tip gate, the $I-V$ is symmetric. In the presence of the tip, the $I-V$ becomes strongly asymmetric, with the forward bias direction determined only by the position of the tip.

We attribute these observations to the formation of back-to-back Schottky barriers at the contacts between the p -type SWNT and the metal electrodes (Fig. 3). Far from the leads, the chemical potential lies near the valence band edge (usual p -type doping due to atmospheric gases and/or charge transfer). At the contacts, charge transfer occurs, and the bands bend down to form Schottky barriers. At zero bias, the barriers have equal height and depletion region width [Fig. 3(a)]. Under applied bias, the depletion region at the positively biased electrode increases (reverse bias) while the other decreases [Fig. 3(b)]. The reverse-biased Schottky barrier at the positive electrode now is the bottleneck for the transport current. Bringing the negatively biased SGM tip near this barrier induces holes in the area and suppresses the Schottky barrier, increasing the transport current dramatically [Fig. 3(c)].

The gating regions imaged in Figs. 2(a) and 2(b) are about 200 nm in size, full width at half maximum. Since the capacitive coupling between tip and sample is a long-range effect (in contrast to the ångstrom scale tunnel coupling in STM), the actual barrier size is convolved with the tip diameter. Taking this effect into account, we can only set an upper limit for the size of the depletion region of 50 nm. The theory predicts that the size of the depletion region depends on the screening length within the one-dimensional nanotube, varying from less than 10 nm to micrometers as the carrier density decreases.¹⁵

When the tip is placed near one electrode with a negative bias [Fig. 2(c)], it breaks the symmetry of the original device. The Schottky barrier under the tip becomes nearly ohmic, and the resulting $I-V$ curves [Fig. 2(c), open triangles and filled circles] are rectifying and reflect the ungated Schottky barrier. We observe as much as a fourfold increase in current for gating at the appropriate contact. The forward-bias region of the $I-V$ extrapolates back to a V

intercept of about 150 meV, which serves as an estimate of the Schottky barrier height. At low bias voltage, the leakage current through the reverse-biased Schottky barrier corresponds to a conductance $G = 1 \mu\text{S}$ or, equivalently, a barrier transparency $T = G/(4e^2/h) = 6 \times 10^{-3}$. This value agrees with the findings of other groups,¹⁶ as well as theoretical predictions²⁵ for doped nanotubes.

The proposed band structure in Fig. 3(a) clarifies all our TUBEFET observations. A negative backgate voltage increases the hole density everywhere in the device, but the areas where the increase matters most are near the contacts where the added carriers reduce the width and height of Schottky barriers. A positive gate voltage has an important effect along the length of the nanotube, and can cause local depletion in regions where electrostatic fluctuations (defects, trapped charges, etc.) bring the valence band edge close to the Fermi level.^{17,18} An overall reduction in the carrier density of the nanotube also increases the screening length and the Schottky barrier depletion widths.¹⁴

In conclusion, through gating with a scanned local probe we have shown that Schottky barriers form at the metal contacts to semiconducting nanotubes, and that the initially symmetric device (metal-semiconductor-metal) can be electrostatically doped to become a diode. The possibility of local gating is not limited to an AFM tip, but could be done with electron accepting impurities.⁵ If such impurities could be selectively introduced near one contact, diodes made of single nanotubes might be reliably engineered.

The authors thank the Smalley Group (Rice University) for laser-ablation grown SWNT samples and Jason Hafner (Harvard) for sharing his expertise in CVD-growth of SWNTs. This work was supported by the National Science Foundation (Grant No. 98-02560), and the Laboratory for Research on the Structure of Matter (a NSF MRSEC, DMR00-79909). W.F.S. thanks the LRSM for support during his sabbatical.

¹N. Hamada, S. Sawada, and A. Oshiyama, *Phys. Rev. Lett.* **68**, 1579 (1992).

- ²R. Saito, M. Fujita, G. Dresselhaus, and M. S. Dresselhaus, *Appl. Phys. Lett.* **60**, 2204 (1992).
- ³J. W. Mintmire, B. I. Dunlap, and C. T. White, *Phys. Rev. Lett.* **68**, 631 (1992).
- ⁴S. J. Tans, A. R. M. Verschueren, and C. Dekker, *Nature (London)* **393**, 49 (1998).
- ⁵R. D. Antonov and A. T. Johnson, *Phys. Rev. Lett.* **83**, 3274 (1999).
- ⁶C. Zhou, J. Kong, and H. Dai, *Science* **290**, 1552 (2000).
- ⁷M. Bockrath, D. H. Cobden, P. L. McEuen, N. G. Chopra, A. Zettl, A. Thess, and R. E. Smalley, *Science* **275**, 1922 (1997).
- ⁸S. J. Tans, M. H. Devoret, H. Dai, A. Thess, R. E. Smalley, L. J. Geerlings, and C. Dekker, *Nature (London)* **386**, 474 (1997).
- ⁹L. Chico, V. H. Crespi, L. X. Benedict, S. G. Louie, and M. L. Cohen, *Phys. Rev. Lett.* **76**, 971 (1996).
- ¹⁰Z. Yao, H. W. C. Postma, L. Balents, and C. Dekker, *Nature (London)* **402**, 273 (1999).
- ¹¹P. G. Collins, K. Bradley, M. Ishigami, and A. Zettl, *Science* **287**, 1801 (2000).
- ¹²R. S. Lee, H. J. Kim, J. E. Fischer, A. Thess, and R. E. Smalley, *Nature (London)* **402**, 273 (1999).
- ¹³M. Bockrath, J. Hone, A. Zettl, P. L. McEuen, A. G. Rinzier, and R. E. Smalley, *Phys. Rev. B* **61**, R10606 (2000).
- ¹⁴R. S. Lee, H. J. Kim, J. E. Fischer, J. Lefebvre, M. Radosavljevic, J. Hone, and A. T. Johnson, *Phys. Rev. B* **61**, 4526 (2000).
- ¹⁵F. Leonard and J. Tersoff, *Phys. Rev. Lett.* **83**, 5174 (1999).
- ¹⁶M. S. Fuhrer, J. Nygard, L. Shih, M. Forero, Y. G. Yoon, M. S. C. Mazzoni, H. J. Choi, J. Ihm, S. G. Louie, A. Zettl, and P. L. McEuen, *Science* **288**, 494 (2000).
- ¹⁷M. Freitag, M. Radosavljevic, W. Clauss, and A. T. Johnson, *Phys. Rev. B* **62**, R2307 (2000).
- ¹⁸S. J. Tans and C. Dekker, *Nature (London)* **404**, 834 (2000).
- ¹⁹A. Bachtold, M. S. Fuhrer, S. Plyasunov, M. Forero, E. H. Anderson, A. Zettl, and P. L. McEuen, *Phys. Rev. Lett.* **84**, 6082 (2000).
- ²⁰M. Bockrath, W. Liang, D. Bozovic, J. H. Hafner, C. M. Lieber, M. Tinkham, and H. Park, *Science* **291**, 283 (2001).
- ²¹J. H. Hafner, C. L. Cheung, and C. M. Lieber, *J. Am. Chem. Soc.* **121**, 9750 (1999).
- ²²Although the CVD-process predominantly yields single wall carbon nanotubes, some multiwall nanotubes with very few (2 or 3) shells might also be present. SWNTs are selected by their apparent height of 2 nm or less in the AFM.
- ²³Data are taken with an Omicron/Zeiss Beetle AFM with a quartz "needle sensor." Tungsten-carbide tips are mounted on the needle sensor and used as conducting probes.
- ²⁴W. Clauss, J. Zhang, D. J. Bergeron, and A. T. Johnson, *J. Vac. Sci. Technol.* **17**, 1309 (1999).
- ²⁵A. A. Odintsov, *Phys. Rev. Lett.* **85**, 150 (2000).